Inter*net* Electronic Journal of

Molecular Design

Three–dimensional Pharmacophore Hypotheses of Octopamine Receptor Responsible for the Inhibition of Sex–pheromone Production in *Plodia interpunctella*

Akinori Hirashima,[1] Tomohiko Eiraku,[2] Eiichi Kuwano,[1] Eiji Taniguchi,[3] and Morifusa Eto[4]

[1] Division of Bioresource and Bioenvironmental Sciences, Graduate School, Kyushu University, Fukuoka 812–8581, Japan
[2] Graduate School of Bioresource and Bioenvironmental Sciences, Kyushu University, 6–10–1 Hakozaki, Higashi–ku, Fukuoka 812–8581, Japan
[3] School of Agriculture, Kyushu Tokai University, Kumamoto 869–1404, Japan
[4] Kyushu Women's University, 1–1 Jiyugaoka, Yahatanishi–ku, Kita–Kyushu, Fukuoka 807–8586, Japan

Citation of the article:
A. Hirashima, T. Eiraku, E. Kuwano, E. Taniguchi, and M. Eto, Three–dimensional Pharmacophore Hypotheses of Octopamine Receptor Responsible for the Inhibition of Sex–pheromone Production in *Plodia interpunctella*, *Internet Electron. J. Mol. Des.* **2002**, *1*, 37–51, http://www.biochempress.com.

Three–dimensional Pharmacophore Hypotheses of Octopamine Receptor Responsible for the Inhibition of Sex–pheromone Production in *Plodia interpunctella*[#]

Akinori Hirashima,[1,]* Tomohiko Eiraku,[2] Eiichi Kuwano,[1] Eiji Taniguchi,[3] and Morifusa Eto[4]

[1] Division of Bioresource and Bioenvironmental Sciences, Graduate School, Kyushu University, Fukuoka 812–8581, Japan
[2] Graduate School of Bioresource and Bioenvironmental Sciences, Kyushu University, 6–10–1 Hakozaki, Higashi–ku, Fukuoka 812–8581, Japan
[3] School of Agriculture, Kyushu Tokai University, Kumamoto 869–1404, Japan
[4] Kyushu Women's University, 1–1 Jiyugaoka, Yahatanishi–ku, Kita–Kyushu, Fukuoka 807–8586, Japan

Abstract

Motivation. Our interest in octopaminergic agonists was aroused by the results of QSAR study using various physicochemical parameters as descriptors or receptor surface models. Furthermore, molecular modeling and conformational analysis were performed in Catalyst/Hypo to gain a better knowledge of the interactions between octopaminergic antagonists and OAR3 in order to understand identification of the conformations required for binding activity.

Method. All experiments were conducted on a Silicon Graphics O2, running under the IRIX 6.5 operating system. Hypotheses generation and its functionality is available as part of Molecular Simulations Incorporated's Catalyst/Hypo modeling environment. Molecules were edited using the Catalyst 2D/3D visualizer.

Results. Three–dimensional pharmacophore hypotheses were built from a set of 14 octopamine (OA) agonists responsible for the inhibition of sex–pheromone production in *Plodia interpunctella*. Among the ten chemical–featured models generated by program Catalyst/Hypo, hypotheses including hydrogen–bond acceptor (HBA), hydrophobic (Hp), hydrophobic aromatic (HpAr), and hydrophobic aliphatic (HpAl) features were considered to be important and predictive in evaluating OA agonists. An HBA and four hydrophobic features are the minimum components of an effective OA agonistic binding hypothesis, which resembles the results of binding activity to locust OAR3.

Conclusions. Active agonists mapped well onto all the features of the hypothesis such as HBA, Hp, HpAr, and HpAl features. On the other hand, inactive compounds lacking binding affinity were shown to be poorly capable of achieving an energetically favorable conformation shared by the active molecules in order to fit the 3D chemical feature pharmacophore models.

Keywords. *Plodia interpunctella;* octopamine agonist; receptor hypothesis; Catalyst; pharmacophore; quantitative structure–property relationships.

Abbreviations and notations

AII, 2–(2,6–diethylphenylimino)imidazolidine	HpAr, hydrophobic aromatic
AIO, 2–(arylimino)oxazolidine	Hp, hydrophobic
AIT, 2–(arylimino)thiazolidine	MBO, 2–(3–methylbenzylthio)–2–oxazoline
BAT, 2–(substituted benzylamino)–2–thiazolines	NI, negative ionizable
CDM, chlordimeform	OA, octopamine
DIP, 2–(2,6–diethylphenylimino)piperidine	PBAN, pheromone biosynthesis activating neuropeptide
HBA, hydrogen–bond acceptor	PI, positive ionizable
HBAl, hydrogen–bond acceptor aliphatic	QSAR, quantitative structure–activity relationships
HBD, hydrogen–bond donor	RA, ring aromatic
HpAl, hydrophobic aliphatic	RMS, root mean square

1 INTRODUCTION

Production of the pheromone blend is under the regulation of a neuropeptide termed pheromone biosynthesis activating neuropeptide (PBAN) [1–4]. The direct action of PBAN has been demonstrated by studies *in vitro* [5–10] showing stimulation of pheromone production in the presence of synthetic peptide by isolated pheromone gland tissue. The exact tissue involved was delineated as the intersegmental membrane that is situated between the 8th and 9th abdominal segments [11,12]. In *Helicoverpa armigera*, we have shown that octopamine (OA) and clonidine significantly inhibit the pheromonotropic action due to PBAN in intact moths and decapitated moths, as well as pheromone gland incubations *in vitro* [11–13]. The inhibition was also reflected in a significant inhibitory effect on intracellular cAMP levels that were stimulated in the presence of PBAN. This inhibitory action is a result of a receptor (separate from the PBAN–receptor) that can be inhibited by pertussis toxin [12]. This provided evidence that this specific pheromonostatic–aminergic receptor is linked to a G–inhibitory protein. Female moths call conspecific males during specific periods when they emit their pheromone. The major pheromone component of Indian meal moth *Plodia interpunctella* was identified as (*Z,E*)–9,12–tetradecadienyl acetate [14–16] and the inhibitors of pheromone production have been reported [17].

The biogenic monoamine OA, which has been found in high concentrations in various insect tissues, is the monohydroxylated analogue of the vertebrate hormone noradrenaline. It has been found that OA is present in a high concentration in various invertebrate tissues [18]. This multifunctional and naturally occurring biogenic amine has been well studied and established as 1) a neurotransmitter, controlling the firefly light organ and endocrine gland activity in other insects; 2) a neurohormone, inducing mobilization of lipids and carbohydrates; 3) a neuromodulator, acting peripherally on different muscles, fat body, and sensory organs such as corpora cardiaca and the corpora allata, and 4) a centrally acting neuromodulator, influencing motor patterns, habituation, and even memory in various invertebrate species [19,20]. The action of OA is mediated through various receptor classes that is coupled to G–proteins and is specifically linked to an adenylate cyclase. Thus, the physiological actions of OA have been shown to be associated with elevated levels of cyclic AMP [21]. Three different receptor classes OAR1, OAR2A, and OAR2B have been

distinguished from non–neuronal tissues [22]. In the nervous system of locust, a particular receptor class was characterized and established as a new class OAR3 by pharmacological investigations of the [^{3}H]OA binding site using various agonists and antagonists [23–27]. Recently much attention has been directed at the octopaminergic system as a valid target in the development of safer and selective pesticides [28–30]. Structure–activity studies of various types of OA agonists and antagonists were reported using the nervous tissue of the migratory locust, *Locusta migratoria* L. [23–27]. However, information on the structural requirements of these OA–agonists and antagonists for high OA–receptor ligands is still limited. The pheromonostatic receptor, acting in a neuromodulatory role, represents a novel type of octopaminergic receptor that induces an inhibitory and not a stimulatory action on adenylate cyclase. It is therefore of critical importance to provide information on the pharmacological properties of this OA receptor types and subtypes.

Our interest in octopaminergic agonists was aroused by the results of quantitative structure–activity relationships (QSAR) study using various physicochemical parameters as descriptors [31,32] or receptor surface models [33]. Furthermore, molecular modeling and conformational analysis were performed in Catalyst/Hypo [34] to gain a better knowledge of the interactions between octopaminergic antagonists [35] and OAR3 in order to understand identification of the conformations required for binding activity. Similar procedure was repeated using OA agonists [36]. The current work is aimed to identify specific and sensitive inhibitors of pheromone biosynthesis in the moth *P. interpunctella*. Three dimensional chemical function–based hypotheses are generated from some set of OA agonists responsible for the inhibition of sex–pheromone production in *P. interpunctella*.

2 MATERIALS AND METHODS

2.1 Synthesis of OA Agonists

The compounds reported here have been prepared according to the Ref. 17. 2–(Arylimino)oxazolidines (AIOs) **1–11** were obtained by cyclodesulfurizing the corresponding thiourea with yellow mercuric oxide. 2–(Arylimino)thiazolidines (AITs) **12–18** and 2–(substituted benzylamino)–2–thiazolines (BATs) **18–20** were synthesized by cyclization of the corresponding thiourea with conc. hydrogen chloride. 2–(2,6–Diethylphenylimino)imidazolidine (AII) **22** was prepared by refluxing the corresponding aniline and 1–acetyl–2–imidazolidone in phosphoryl chloride followed by hydrolysis. 2–(3–Methylbenzylthio)–2–oxazoline (MBO) **23** was prepared from oxazolidine–2–thione and *m*–methylbenzylamine in the presence of sodium hydride. 2–(2,6–Diethylphenylimino)piperidine (DIP) **24** was obtained by refluxing δ–valerolactam and the corresponding aniline in phosphoryl chloride. The structures of the compounds were confirmed by ^{1}H and ^{13}C NMR measured with a JEOL JNM–EX400 spectrometer at 400 MHz, tetramethyl silane

(TMS) being used as an internal standard for ^{1}H NMR and by elemental analytical data. Chlordimeform (CDM, 96% pure) **25** was a gift from Nihon Nohyaku Co. Ltd (Osaka, Japan) and used after purification by column chromatography on silica gel.

Table 1. Octopamine Agonists Used in this Study

Compound[a]	R	mp (^{o}C)	IC$_{50}$ (mM)[b]
1	AIO H	132–134	>10
2	AIO 2–CH$_3$	oil	>10
3	AIO 2–CH$_2$CH$_3$	61–63	4.67(3.92–5.56)
4	AIO 2–CH(CH$_3$)$_2$	89–91	6.46(5.66–7.35)
5	AIO 2,6–Cl$_2$	175–176	50
6	AIO 2,6–(CH$_3$)$_2$	oil	50
7	AIO 2–CH$_3$,6–CH$_2$CH$_3$	102–104	3.07(2.14–4.67)
8	AIO 2–CH$_3$,6–CH(CH$_3$)$_2$	oil	5.83(5.40–6.26)
9	AIO 2,6–(CH$_2$CH$_3$)$_2$	172–174	0.28(0.19–0.37)
10	AIO 2–CH$_2$CH$_3$,6–CH(CH$_3$)$_2$	103–105	1.65(1.30–2.05)
11	AIO 2,6–[CH(CH$_3$)$_2$]$_2$	169–170	1.02(0.79–1.29)
12	AIT H	174–176	100
13	AIT 2–CH$_2$CH$_3$	59–61	0.39(026–0.57)
14	AIT 2,4–(CH$_3$)$_2$	106–108	2.12(1.82–2.48)
15	AIT 2,4,6–(CH$_3$)$_3$	99–101	3.03(2.48–3.65)
16	AIT 2,6–(CH$_3$)$_2$	169–171	1.38(1.07–1.75)
17	AIT 2,6–(CH$_2$CH$_3$)$_2$	72–74	0.27(0.18–0.40)
18	AIT 2–CH$_2$CH$_3$,6–CH(CH$_3$)$_2$	138–140	0.82(0.56–1.15)
19	BAT 2–CH$_3$	119–120	50
20	BAT 3–CH$_3$	65–66	2.20(1.81–2.68)
21	BAT 2,3–(OCH$_3$)$_2$	102–103	60
22	AII 2,6–(CH$_2$CH$_3$)$_2$	168–169	4.05(2.66–6.76)
23	MBO	oil	0.097(0.057–0.153)
24	DIP	oil	>10
25	CDM	oil	3.90(3.01–4.90)

[a] AIOs **1**–**11** were obtained by cyclodesulfurizing the corresponding *N*–arylthioureas with yellow mercuric oxide [17]. AITs **12**–**18** and BAT **19**–**21** were synthesized by cyclization of the corresponding *N*–arylthioureas with concentrated hydrogen chloride [32]. AII **22** was prepared according to a reported method by refluxing the corresponding substituted anilines and 1–acetyl–2–imidazolidone in phosphoryl chloride followed by hydrolysis [17]. MBO **23** was prepared from oxazolidine–2–thione and *m*–methylbenzylamine in the presence of sodium hydride. DIP **24** was obtained by refluxing δ–valerolactam and the corresponding aniline in phosphoryl chloride. In parentheses, 95% confidence limit values are shown.
[b] The intersegments of *P. interpunctella* were incubated individually in 10 μl medium containing 0.5 μCi [1–^{14}C]acetate in the presence of synthetic Hez–PBAN (0.5 μM) and test compounds at room temperature for 3 h, maintaining the photoperiod. In order to measure the incorporation of [1–^{14}C]acetate into pheromone components, the glands were extracted in hexane, which was washed with water, and the amount of radioactivity of the hexane extract was measured using a LSC after adding scintillation cocktail. The response obtained in control pheromone gland incubated with Hez–PBAN (0.5 μM) alone is regarded as 100%.

2.2 Insect Culture

The colony of *P. interpunctella* was raised on a diet of 80% ground rice, 10% glycerin, 5% brewer's yeast, and 5% honey at 28°C and 70% RH in a 14:10 (light:dark) photoperiod as reported previously [37]. Larvae of wandering stage were pupated between pieces of paper carton and the resulting pupae were sexed and males and females were emerged separately. Emerged virgin females were staged according to age.

http://www.biochempress.com
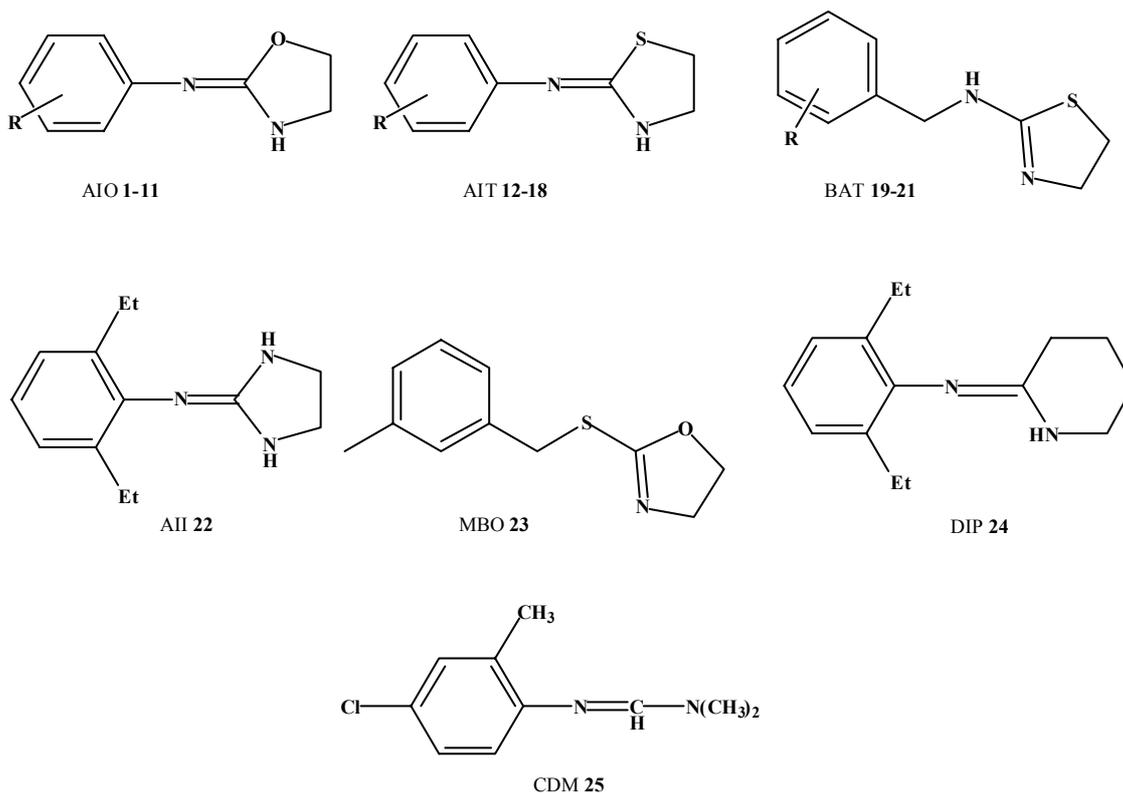
Figure 1. Structures of octopamine agonists in the training and test sets.

2.3 *In vitro* Pheromone–Production Bioassay

Compounds were tested for inhibitory specificity using a modified radiochemical bioassay to monitor *de novo* pheromone production [17]. Abdominal tips, containing the eighth and ninth abdominal segments with the attached intersegmental membrane, were removed from 1 day–old virgin females under sterile conditions during the first–third hour scotophase, using a dim red light for illumination. After preincubation in Pipes–buffered incubation medium [38] for 30 min, the intersegments were dried on tissue paper and then transferred individually to 10 μl medium containing 0.5 μCi [1–^{14}C]acetate in the presence or absence of 0.5 μM synthetic Hez–PBAN and test compounds. All incubations for pheromone production were performed at room temperature, maintaining the photoperiod. After the required incubation period (3 h) in order to measure the incorporation of [1–^{14}C]acetate into pheromone components, the glands were extracted in hexane, which was washed with water, and the amount of radioactivity of the hexane extract was measured using a liquid scintillation counter (LSC, Beckman LS 6500 multipurpose liquid scintillation analyzer) after adding scintillation cocktail (Clear–sol I).

2.4 Statistical Analysis

In the experiments, differences between two treatments were compared by Student's *t* test and those among three or more treatments were analyzed by One–way Factorial ANOVA followed by

Scheffe test as Post–Hoc Test. All differences, unless otherwise noted, are reported at $P < 0.05$.

2.5 Computational Details

2.5.1 Hypothesis generation

All experiments were conducted on a Silicon Graphics O2, running under the IRIX 6.5 operating system. Hypotheses generation and its functionality is available as part of Molecular Simulations Incorporated's Catalyst/Hypo modeling environment. Molecules were edited using the Catalyst 2D/3D visualizer. The Catalyst model treats molecular structures as templates consisting of strategically positioned chemical functions that will bind effectively with complementary functions on receptors. The biologically most important binding functions are deduced from a small set of compounds that cover a broad range of activity. Catalyst automatically generated conformational models for each compound using the Poling Algorithm [39–41]. Diverse conformational models for each compound were generated such that the conformers covered accessible conformational space defined within 20 kcal of the estimated global minimum. The models emphasized a conformational diversity under the constraint energy threshold above the estimated global minimum based on use of the CHARMm force field [39–42]. Molecular flexibility is taken into account by considering each compound as a collection of conformers representing a different area of conformational space accessible to the molecule within a given energy range. Catalyst provides two types of conformational analysis: fast and best quality. Fast option was used, specifying 250 as the maximum number of conformers.

The molecules associated with their conformational models were submitted to Catalyst hypothesis generation. The present work shows how a set of binding activities of various OA agonists, responsible for the inhibition of sex–pheromone production in *P. interpunctella*, may be treated statistically to uncover the molecular characteristics that are essential for high activity. These characteristics are expressed as chemical features disposed in three–dimensional space and are collectively termed a hypothesis. Hypotheses approximating the pharmacophore are described as a set of features distributed within a 3D space. This process only considered surface accessible functions such as hydrogen–bond acceptor (HBA), hydrogen–bond acceptor aliphatic (HBAl), hydrogen–bond donor (HBD), hydrophobic (Hp), hydrophobic aromatic (HpAr), hydrophobic aliphatic (HpAl), negative charge, positive charge, ring aromatic (RA), negative ionizable (NI), and positive ionizable (PI) [43]. A preparative test was performed with these features. NI and PI were used rather than negative charge and positive charge in order to broaden the search for deprotonated and protonated atoms or groups at physiological pH. Furthermore, in order to emphasize the importance of an aromatic group corresponding to the phenol moiety of test compounds, RA that consists of directionality was chosen to be included in the subsequent run. The hypothesis generator was restricted to select only five features due to the molecule's flexibility and functional

complexity. For molecules larger than dipeptides, Catalyst often will find five–feature hypotheses automatically, but for smaller molecules, three– or four–feature hypotheses might be in the majority. Since hypotheses with more features are more likely to be stereospecific and generally more restrictive models, the total features minimum value was set to 5 in order to force Catalyst to search for 5–feature hypotheses [31].

2.5.2 Validation of the hypothesis

During a hypothesis generation run, Catalyst considers and discards many thousands of models. It attempts to minimize a cost function consisting of two terms. One penalizes the deviation between the estimated activities of the training set molecules and their experimental values. The other penalizes the complexity of the hypothesis. The overall assumption used is based on Occam's razor, that between otherwise equivalent alternatives, the simplest model is best. Simplicity is defined using the minimum description length principle from information theory. The overall cost of a hypothesis is calculated by summing the cost function consisting of three terms (weight cost, error cost, and configuration cost). Weight cost is a value that increases in a Gaussian form as the feature weight in a model deviates from an idealized value of 2.0. Error cost is a major value that increases as root mean square (RMS) difference between estimated and measured activities. Configuration cost is a fixed cost that depends on the complexity of the hypothesis, equal to entropy of the hypothesis space.

Besides providing a numerical score for each generated hypothesis, Catalyst provides two numbers to help the chemist assess the validity of a hypothesis. One is the cost of an ideal hypothesis, which is a lower bound on the cost of the simplest possible hypothesis that still fits the data perfectly. The other is the cost of the null hypothesis, which presumes that there is no statistically significant structure in the data, and that the experimental activities are normally distributed about their mean. Generally, the greater the difference between the two costs, the higher the probability for finding useful models. In terms of hypothesis significance, a generated hypothesis with a cost that is substantially below that of the null hypothesis is likely to be statistically significant and bears visual inspection [44].

3 RESULTS AND DISCUSSION

3.1 Assessment of 3D–QSAR for Inhibitory Activity

A set of 14 molecules, that are responsible for the inhibition of sex–pheromone production in *P. interpunctella*, was selected as the target training set. Their chemical structures and experimental activities are listed in Figure 1 and Table 1. MBO **23** had the highest potency, followed by AIT derivative substituted with 2,6–$(CH_2H_3)_2$ **17** and AIO **10** in inhibition of *de novo* pheromone production (Table 1). Affinities of the agonists are expressed as their IC_{50} values in mM and

activities range over three orders of magnitude (min. 0.097 mM and max. 100 mM). This set included a variety of types of molecules and for this type of training set, the use of the hypothesis generation tool was appropriate. This tool builds hypotheses (overlays of chemical features) for which the fit of individual molecules to a hypothesis can be correlated with the molecule's affinity.

The 3D–QSAR study was performed with the Catalyst (Version 4.0) package. The geometry of each compound was built with a visualizer and optimized by using the generalized CHARMm–like force field [39–42] implemented in the program. It was found that hypotheses contain good correlation with HBA, Hp, HpAr, and HpAl. The characteristics (cost, RMS, and the regression constant *r*) of the ten lowest cost hypotheses are listed in Table 2. The statistical relevance of the various hypotheses obtained is assessed on the basis of their cost relative to the null hypothesis and their correlation coefficients *r* [31]. The total fixed cost of the run is 58.63 and the cost of the null hypothesis is 67.61. The cost range between best hypothesis 1 and null hypothesis is 1.79. The cost range over the 10 generated hypotheses is 1.47. Hypotheses 2 and 3 consist of the same chemical–feature functions as an HBAl, an Hp, two HpAls, and an HpAr feature.

3.2 Validation of the Hypothesis

The hypotheses are used to estimate the activities of the training set. Those activities are derived from those conformers displaying the smallest RMS deviations when projected onto the hypothesis. Hypotheses 1–10 shared five common features located at almost exactly the same 3D coordinates. The quality of the correlation among the data in the training set is given by the RMS score that was normalized by the log (uncertainty) and *r*. All calculated activities from 10 best hypotheses and the number of generated conformations for each molecule are listed in Table 2. Even though hypothesis 1 has a lower cost value than others and the RMS index for hypothesis 1 is very small as 0.880, they have nearly no difference in *r* and RMS (Table 3).

Table 2. Predicted Activity from 10 Best Hypotheses against Actual Inhibitory Activity Data for 14 Agonists

Comp.	Exp.[a]	Conf.[a]	Hypotheses									
No.	(mM)		1	2	3	4	5	6	7	8	9	10
1	>10	2	74	67	83	120	81	60	66	90	83	80
2	>10	4	23	18	20	11	14	16	16	17	18	16
3	4.67	6	3.8	5	8.8	13	13	14	8.2	8.4	8.9	13
7	3.07	6	2.3	1.1	2	2.1	2.5	0.98	1.2	1.3	1.2	1.3
9	1.65	9	0.7	0.9	0.65	1.1	0.74	0.84	1	0.85	0.82	0.8
10	0.28	14	1.3	1.3	1.1	1.3	2.2	1.2	1.3	1.1	1.1	1.2
11	1.02	12	2.7	2.2	2.3	1.2	0.99	1.5	1.8	1.8	1.7	1.7
14	2.12	4	1.8	2.8	1.5	4.4	4.3	3	3.6	4.3	5.3	4.7
16	1.38	6	4.7	3.4	3.8	0.67	1.2	2.4	2.2	2.5	2.4	2.7
17	0.27	11	0.71	0.9	0.65	1.4	1.2	0.84	1.3	0.83	0.81	0.77
20	2.20	10	2.3	2.8	2	1.8	1.7	2.6	1.8	3.3	3	2.5
22	4.05	25	2.4	3.4	2	1.6	1.3	3	3	25	2.4	2.3
23	0.097	29	0.016	0.014	0.02	0.028	0.027	0.018	0.014	0.015	0.015	0.017
25	3.90	3	7.7	7.5	3.1	6.6	6.5	8.2	6.8	4.8	5.1	4.7

[a] Abbreviations: Exp., experimental data (I_{50} in mM for inhibition of pheromone production); Conf., number of conformational models.

http://www.biochempress.com

Table 3. Characteristics of Ten Lowest Cost Hypotheses from 14 OA Agonists (Cost of Ideal Hypothesis: 58.63, Cost of Null Hypothesis: 67.61)

Hypotheses	Feature[a]					Cost	RMS	r
	1	2	3	4	5			
1	HBA	Hp	Hp	HpAl	HpAr	65.83	0.880	0.865
2	HBAl	Hp	HpAl	HpAl	HpAr	66.57	0.930	0.848
3	HBAl	Hp	HpAl	HpAl	HpAr	66.59	0.882	0.866
4	HBA	Hp	Hp	Hp	Hp	66.89	0.950	0.840
5	HBAl	Hp	Hp	Hp	Hp	66.93	0.986	0.825
6	HBAl	HpAl	HpAl	HpAl	HpAr	67.08	0.929	0.849
7	HBA	Hp	HpAl	HpAl	HpAr	67.08	0.940	0.844
8	HBA	HBA	Hp	HpAl	HpAl	67.08	0.887	0.865
9	HBA	HBAl	Hp	HpAl	HpAl	67.12	0.884	0.866
10	HBAl	HBAl	Hp	HpAl	HpAr	67.30	0.910	0.856

[a] Abbreviations: HBA, hydrogen–bond acceptor; HBAl, hydrogen–bond acceptor aliphatic; Hp, hydrophobic; HpAl, hydrophobic aliphatic.

Roughly speaking, the greater the difference between the cost of the generated hypothesis and that of the null hypothesis, the more likely it is that the hypothesis reflects a chance correlation [42]. The correlation between observed and estimated inhibitory activities is satisfactory in the three hypotheses. The predicted activities are in the right order and parallel the values actually observed (Table 2).

The small cost range observed here might be due to two factors, namely molecules in the training set are fairly rigid and have a high degree of structural homology. Due to the relatively small range between the costs for an ideal versus null hypothesis and due moreover to the placement of the identified hypotheses within this range, special care was taken to test for chance correlation. The hypothesis 1 turns out to be the best measure in the test set for the whole training set as attested by the reasonably good correlation between observed and estimated activities (cost = 65.83, cost of the null hypothesis = 67.61). Hence, the hypothesis 1 was regressed using each molecule in its most chemically reasonable conformation. Compounds **10**, **11**, **16**, **17**, and **25** were underestimated by hypothesis 1, which had the highest statistical correlation (r = 0.865) and the smallest error value (RMS = 0.880). The number of compounds used in preparing Catalyst hypothesis is still small (only 14), that it will need improvement to design new molecules.

3.3 Receptor–Drug Interaction

QSAR modeling is an area of research pioneered by Hansch and Fujita [45,46]. QSAR attempts to model the activity of a series of compounds using measured or computed properties of the compounds. More recently, QSAR has been extended by including the three–dimensional information. In drug discovery, it is common to have measured activity data for a set of compounds acting upon a particular protein but not to have knowledge of the three–dimensional structure of the active site. In the absence of such three–dimensional information, one can attempt to build a hypothetical model of the receptor site that can provide insight about receptor site characteristics. Such a model is known as a Hypo, which provides three–dimensional information about a putative

receptor site. Catalyst/Hypo was useful in building 3D pharmacophore models from the binding activity data and conformational structure. It can be used as an alternative for QSAR methods.
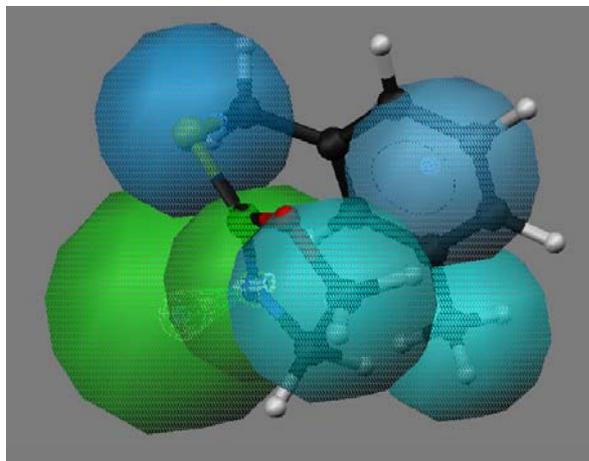
Figure 2. Mapping of **23** onto hypothesis 1, which contains an HBA (green), two Hps (light blue), an HpAr (blue), and an HpAl (dark blue).
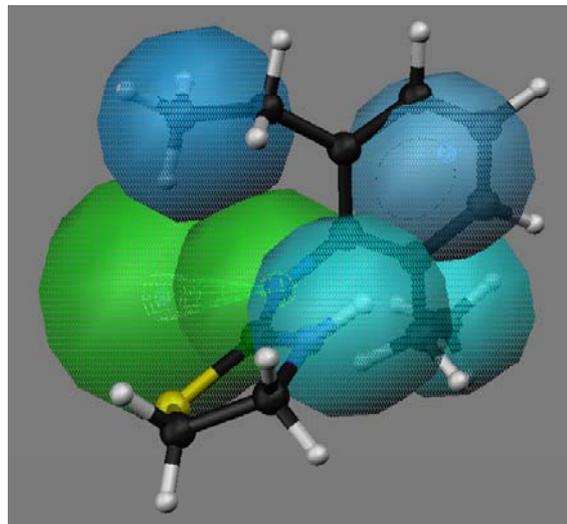
Figure 3. Mapping of **17** onto hypothesis 1, which consists of an HBA (green), two Hps (light blue), an HpAr (blue), and an HpAl (dark blue).
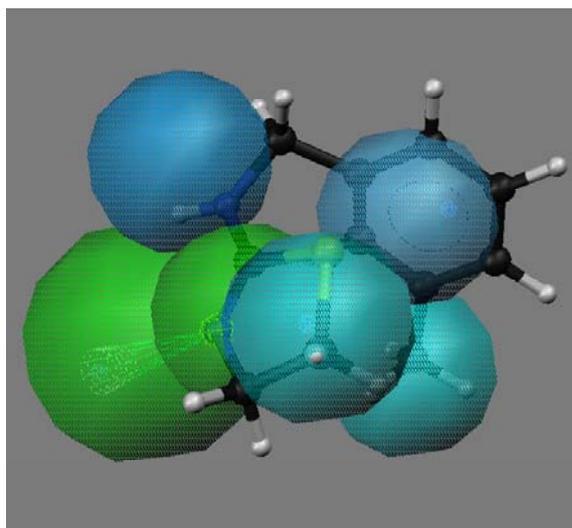
Figure 4. Mapping of **20** onto hypothesis 1, which consists of an HBA (green), two Hps (light blue), an HpAr (blue), and an HpAl (dark blue).
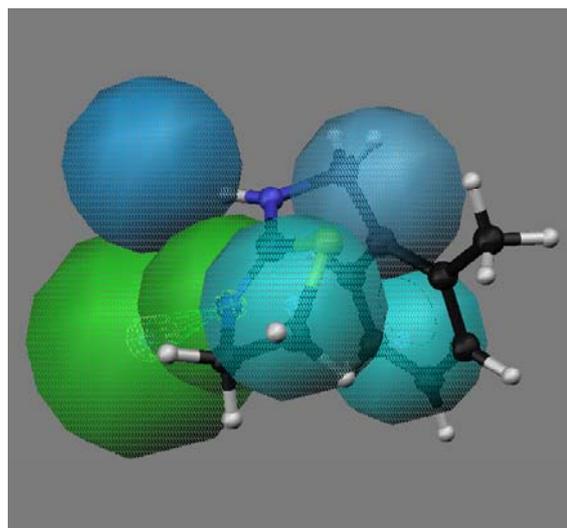
Figure 5. Mapping of **19** onto hypothesis 1, which consists of an HBA (green), two Hps (light blue), an HpAr (blue), and an HpAl (dark blue).

Figure 2 depicts one of the most active conformations of MBO **23** in the training set mapped onto the lowest cost hypothesis 1. The phenyl group of **23** overlaps with the HpAr feature of hypothesis 1, whereas the nitrogen atom of oxazolidine ring serves as an HBA. The pair of Hp features overlap neatly with the methyl and methylenethio groups, respectively, and an HpAl is disposed over the oxazolidine ring. Thus, the most active OA agonist **23** in the training set maps closely with the statistically most significant hypothesis 1, which is characterized by five features

(Figure 2) and the predicted activity of **23** by hypothesis 1 is reasonable (Table 2). Meanwhile, AIO with shorter bridge between phenyl and oxazoline rings than MBO is suitable for the hypothesis (Figure 3). The phenyl group of **17** overlaps with the HpAr feature of hypothesis 1, whereas the bridge nitrogen atom serves as an HBA, between a phenyl and thiazolidine rings (Figure 3). The pair of Hp features overlaps neatly with the two ethyls of 2,6–diethyl group, respectively, and an HpAl is disposed over the thiazolidine ring. AIO **17** has a phenyl and oxazolidine ring directly connected by nitrogen and thus, is less flexible than MBO, because **17** has less (11) conformational flexibility than that (29) of **23**. The molecule map well onto all five hypotheses features in a similar way in hypotheses 1–10 (data not shown) and therefore these hypotheses are considered to be equivalent. Roughly speaking, hypotheses 1–10 have good similarity in 3D spatial shape.

Although BAT **20** (Figure 4) fit five features of hypothesis 1 in a similar way as BMO **23** (Figure 2), the methyleneamino group (hydrophobic parameter [46] π, –0.47) of **20** is less hydrophobic than the methylenethio group of **23** (π, 0.61) and thus, **20** is less active than **23** (Table 1). BAT **20** with the lowest activity in the training set (exp. 2.2 mM) fits only two features of hypothesis 1 (Figure 4) and thus, **20** is less active than **19** (Figure 5). Thus, the present studies on OA agonists demonstrate that an HBA site and four hydrophobic sites located on the molecule seem to be essential in inhibition of pheromone production of *P. interpunctella*. The result resembles that of binding activity to locust OAR3 [36], in which an HBA site and four hydrophobic sites located on the molecule also seem to be essential in binding of OA agonists to OAR3. The phenyl moiety, 4–substituent, and imidazolidine ring of the most active compound as OA agonist to OAR3 overlaps with the three Hp features of hypothesis 1, whereas the bridge nitrogen atom, between a phenyl and imidazolidine rings, serves as an HBA. The HpAl feature overlaps neatly with the 2–substituent. Generally, more active molecules map onto all the features of the hypothesis. Conversely, compounds that are estimated to have low activity map poorly to the hypothesis.

Table 4. Predicted Activity of OA Agonists from Hypothesis 1

Compound	Conf.[a]	IC$_{50}$ (mM)		Error[b]
		Experimental	Predicted	
4	5	6.46	12	1.8
5	14	50	4.7	–11
6	6	50	4.7	–11
8	12	5.83	4.9	–1.2
12	2	100	81	–1.2
13	5	0.39	7.5	19
15	10	3.03	3.3	1.1
18	7	0.82	0.78	–1.1
19	3	50	10	–4.9
21	18	50	1.7	–35
24	15	100	1.9	–53

[a] Conf. denotes the number of conformational models.
[b] The error is computed by dividing the predicted activity by the experimental value when the predicted activity is underestimated, and by dividing the experimental activity by the predicted value and adding a minus sign to the result when the predicted activity is overestimated.

The predictive character of this five–feature hypothesis was further assessed using candidate molecules, whose structures are shown in Figure 1, outside of the training set (Table 4). The best statistically significant hypothesis 1 was applied to access the activities of those OA agonists and the predicted values of the most active molecules are listed in Table 4. The predicted activity of **5**, according to hypothesis 1, was 4.7 mM and that of experimental value was 50 mM. One of the reasons why this prediction is so bad may be that **5** in the only compound with halogen substituent used in preparing Catalyst hypothesis. Thus, it will need improvement to design new molecules. It is necessary to include various types of compounds with variety of activity to obtain better hypothesis and predictions before designing new molecules in the future. Thus, the hypothesis 1 is considered for further use in designing new leads for hopefully more active compounds. Thus, further research on the comparison of the 3D hypotheses from more potent OA agonists as well as those generated from the corresponding data from various insect might be interesting and stimulating to investigate further the mechanisms of OA receptor–ligand interactions.

4 CONCLUSIONS

Three–dimensional pharmacophore hypotheses were built from a training set of 14 OA agonists. Hypotheses were obtained from this study and applied to map with the active or inactive compounds to explain the mechanism of OA receptor–ligand interactions. Important features were found such as HBA, Hp, HpAr, and HpAl of the surface–assessable models. An HBA and four hydrophobic features are the minimum components of an effective OA agonistic binding hypothesis, which resembles the results of binding activity to locust OAR3. It was found that more active agonists map well onto all the features of the hypotheses, meanwhile for some inactive compounds, their lack of binding affinity is primarily due to their inability to achieve an energetically favorable conformation shared by the active compounds in order to fit the 3D common feature pharmacophore keys.

Based upon this study, several three–dimensional pharmacophore models for the OA agonists–receptor interactions have been proposed. Those hypotheses are considered to be useful in designing new leads for hopefully more active compounds, although the numbers of compounds tested are still limited. Hence, a further comparison study of 3D hypothesis models of agonists responsible for the inhibition of sex–pheromone production in *P. interpunctella* is in progress and expected to clarify the mode of action of these compounds acting on the OA receptor. Such work will surely help elucidate the mechanisms of OA receptor–ligand interactions. The above hypotheses studies show that agonists with certain substituents can be potential ligands to OA receptors. They may help to point the way towards developing extremely potent and relatively specific OA agonists, leading to potential pest–control agents. In order to optimize the activities of these compounds as OA–agonists, more detailed experiments are in progress.

Acknowledgment

5 REFERENCES

[1] A. K. Raina, Neuroendocrine control of sex pheromone biosynthesis in Lepidoptera, *Ann. Rev. Entomol.* **1993**, *38*, 329–349.

[2] P. W. K. Ma and W. Roelofs, Calcium involvement in the stimulation of sex pheromone production by PBAN in the European Corn Borer, *Ostrinia nubilalis* (Lepidoptera: Pyralidae), *Insect Biochem. Mol. Biol.* **1995**, *25*, 467–473.

[3] A. Rafaeli and C. Gileadi, Neuroendocrine control of pheromone production in moths, *Invert. Neurosci.* **1997**, *3*, 223–229.

[4] R. A. Jurenka, Signal transduction in the stimulation of sex pheromone biosynthesis in moths, *Arch. Insect Biochem. Physiol.* **1996**, *33*, 245–258.

[5] V. Soroker and A. Rafaeli, *In vitro* hormonal stimulation of acetate incorporation by *Heliothis armigera* pheromone glands, *Insect Biochem.* **1989**, *19*, 1–9.

[6] A. Rafaeli, V. Soroker, B. Kamensky, and A. K. Raina, Action of PBAN on *in vitro* pheromone glands of *Heliothis armigera* females, *J. Insect Physiol.* **1990**, *36*, 641–646.

[7] R. Arima, K. Takahara, T. Kadoshima, F. Numazaki, T. Ando, M. Uchiyama, H. Nagasawa, A. Kitamura, and A. Suzuki, Hormonal regulation of pheromone biosynthesis in the silkworm moth *Bombyx mori* (Lepidoptera: Bombycidae), *Appl. Entomol. Zool.* **1991**, *26*, 137–148.

[8] R. A. Jurenka, E. Jacquin, and W. L. Roelofs, Stimulation of pheromone biosynthesis in the moth *Helicoverpa zea*, Action of a brain hormone on pheromone glands involves Ca^{2+} and cAMP as second messengers, *Proc. Natl Acad. Sci. USA* **1991**, *88*, 8621–8625.

[9] A. Fonagy, S. Matsumoto, L. Schoofs, A. De Loof, and T. Mitsui, *In vivo* and *in vitro* pheromonotropic activity of two locustatachykinin peptides in *Bombyx mori*, *Biosci. Biotech. Biochem.* **1992**, *56*, 1692–1693.

[10] S. Matsumoto, R. Ozawa, T. Nagamine, G.–H. Kim, K. Uchiumi, T. Shono, and T. Mitsui, Intracellular transduction in the regulation of pheromone biosynthesis of the silkworm, *Bombyx mori:* Suggested involvement of calmodulin and phosphoprotein phosphatase, *Biosci. Biotech. Biochem.* **1995**, *59*, 560–562.

[11] A. Rafaeli and C. Gileadi, Modulation of the PBAN–induced pheromonotropic activity in *Helicoverpa armigera*, *Insect Biochem. Mol. Biol.* **1995**, *25*, 827–834.

[12] A. Rafaeli and C. Gileadi, Down regulation of pheromone biosynthesis: Cellular mechanisms of pheromonostatic responses, *Insect Biochem Mol. Biol.* **1996**, *26*, 797–807.

[13] A. Rafaeli, C. Gileadi, Y. Fan, and C. Meixun, Physiological mechanisms of pheromonostatic responses: effects of adrenergic agonists and antagonists on moth pheromone biosynthesis, *J. Insect Physiol.* **1997**, *43*, 261–269.

[14] Y. Kuwahara, C. Kitamura, S. Takahashi, H. Hara, S. Ishii, and H. Fukami, Sex pheromone of the almond moth and Indian meal moth: cis–9, trans–12–tetradecadienyl acetate, *Science* **1971**, *171*, 801–802.

[15] U. E. Brady, J. H. Tumlinson, R. G. Brownlee, and R. M. Silverstein, Sex stimulant and attractant in the Indian meal moth and in the almond moth, *Science* **1971**, *171*, 802–804.

[16] J. Zhu, C. Ryne, C. R. Unelinus, P. G. Valeur, and C. Lofstedt, Reidentification of the female sex pheromone of the Indian meal moth *Plodia interpunctella*: evidence for a four–component pheromone blend, *Entomol. Experiment. Appl.* **1999**, *92*, 137–146.

[17] A. Hirashima, T. Eiraku, Y. Watanabe, E. Kuwano, E. Taniguchi, and M. Eto, Identification of novel inhibitors of calling and *in vitro* [^{14}C]acetate incorporation by pheromone glands of *Plodia interpunctella*, *Pest Manag. Sci.* **2001**, *57*, 713–720.

[18] J. Axelrod and J. M. Saavedra, Octopamine, *Nature* **1977**, *265*, 501–504.

[19] P. D. Evans, *Reviews in Comparative Molecular Neurobiology*, Ed. S. R. Heller, Birkhäuser Verlag, Basel, 1993, pp. 287–296.

[20] P. D. Evans, *Reviews in Comprehensive Insect Physiology Biochemistry Pharmacology*, Eds. G. A Kerkut and G. Gilbert, Pergamon Press, Oxford, 1985, Vol 11, pp. 499–530.

[21] J. A. Nathanson, Phenyliminoimidazolidines. Characterization of a class of potent agonists of octopamine–sensitive adenylate cyclase and their use in understanding the pharmacology of octopamine receptors, *Mol. Pharm.* **1985**, 28, 254–268.

[22] P. D. Evans, Multiple receptor types for octopamine in the locust, *J. Physiol.* **1981**, *318*, 99–122.

[23] T. Roeder and J. A. Nathanson, Characterization of insect neuronal octopamine receptors (OA3 receptors),

Neurochem. Res. **1993**, 18, 921–925.

[24] T. Roeder and M. Gewecke, Octopamine receptors in locust nervous tissue. *Biochem. Pharm.* **1990**, *39*, 1793–1797.

[25] T. Roeder, A new octopamine receptor class in locust nervous tissue, the octopamine 3 (OA3) receptor, *Life Science* **1992**, *50*, 21–28.

[26] T. Roeder, Pharmacology of the octopamine receptor from locust central nervous tissue (OAR3), *Br. J. Pharm.* **1995**, *114*, 210–216.

[27] T. Roeder, High–affinity antagonists of the locust neuronal octopamine receptor. *Eur. J. Pharm.* **1990**, *191*, 221–224.

[28] K. R. Jennings, D. G. Kuhn, C. F. Kukel, S. H. Trotto, and W. K. Whiteney, A biorationally synthesized octopaminergic insecticide: 2–(4–chloro–*o*–toluidino)–2–oxazoline, *Pestic. Biochem. Physiol.* **1988**, *30*, 190–197.

[29] A. Hirashima, Y. Yoshii, and M. Eto, Action of 2–aryliminothiazolidines on octopamine–sensitive adenylate cyclase in the American cockroach nerve cord and on the two–spotted spider mite *Tetranycus urticae* Koch, *Pestic. Biochem. Physiol.* **1992**, *44*, 101–107.

[30] S. M. M. Ismail, R. A. Baines, R. G. H. Downer, and M. A. Dekeyser, Dihydrooxadiazines: Octopaminergic system as a potential site of insecticidal action. *Pestic. Sci.* **1996**, *46*, 163–170.

[31] A. Hirashima, K. Shinkai, C. Pan, E. Kuwano, E. Taniguchi, and M. Eto, Quantitative Structure–Activity Studies of Octopaminergic Ligands against *Locust migratoria* and *Periplaneta americana*, *Pestic. Sci.* **1999**, *55*, 119–128.

[32] C. Pan, A. Hirashima, J. Tomita, E. Kuwano, E. Taniguchi, and M. Eto, Quantitative structure–activity relationship studies and molecular modelling of octopaminergic 2–(substituted benzylamino)–2–thiazolines and oxazolines against nervous system of *Periplaneta americana* L., *Internet J. Sci.–Biol. Chem.* **1997**, *1*, http://www.netsci–journal.com/97v1/97013/index.htm.

[33] A. Hirashima, C. Pan, J. Tomita, E. Kuwano, E. Taniguchi, and M. Eto, Quantitative structure–activity studies of octopaminergic agonists and antagonists against nervous system of *Locusta migratoria*, *Bioorg. Med. Chem.* **1998**, *6*, 903–910.

[34] Catalyst Tutorial, Version 4.0, Molecular Simulations Inc., San Diego, CA, 1998.

[35] C. Pan, A. Hirashima, E. Kuwano, and M. Eto, Three–dimensional pharmacophore hypotheses for the locust neuronal octopamine receptor (OAR3): 1. Antagonists, *J. Mol. Model.* **1997**, *3*, 455–463.

[36] A. Hirashima, C. Pan, E. Kuwano, E. Taniguchi, and M. Eto, Three–dimensional pharmacophore hypotheses for the locust neuronal octopamine receptor (OAR3): 2. Agonists, *Bioorg. Med. Chem.* **1999**, *7*, 1437–1443.

[37] A. Rafaeli and C. Gileadi, Factors affecting pheromone production in the stored product moth, *Plodia interpunctella*: a preliminary study, *J. Stored Prod. Res.* **1995**, *31*, 243–247.

[38] A. Rafaeli, C. Gileadi, and A. Hirashima, Identification of novel synthetic octopamine receptor agonists which inhibit moth sex pheromone production, *Pestic. Biochem. Physiol.* **1999**, *65*, 194–204.

[39] A. Smellie, S. L. Teig, and P. Towbin, Poling–promoting conformational variation, *J. Comput. Chem.* **1995**, *16*, 171–187.

[40] A. Smellie, S. D. Kahn, and S. L. Teig, Analysis of conformational coverage. 1. Validation and estimation of coverage, *J. Chem. Inf. Comput. Sci.* **1995**, *35*, 285–294.

[41] A. Smellie, S. D. Kahn, and S. L. Teig, Analysis of conformational coverage. 2. Application of conformational models, *J. Chem. Inf. Comput. Sci.* **1995**, *35*, 295–304.

[42] B. R. Brooks, R. E. Brucolleri, B. D. Olafson, D. J. States, S. Swaminathan, and M. Karplus, CHARMM: A progrm for macromolecular energy, minimization, and dynamics calculations, *J. Comput. Chem.* **1983**, *4*, 187–217.

[43] J. Greene, S. Kahn, H. Savoj, P. Sprague, and S. Teig, Chemical function queries for 3D database search, *J. Chem. Inf. Comput. Sci.* **1994**, *34*, 1297–1308.

[44] R. Hoffmann and J.–J. Bourguignon, Building a Hypothesis for CCK–B Antagonists. 1: Peptoids; In: Complete Listing of Case Studies by Application Area, Molecular Simulations Inc., http://www.msi.com/solutions/cases/notes/CCKB_Pep_full.html.

[45] C. Hansch and A. Leo, Exploring QSAR: Fundamentals and Applications in Chemistry and Biochemistry, American Chemical Society, Washington, DC, 1995.

[46] C. Hansch and T. Fujita, ρ–σ–π Analysis. A method for the correlation of biological activity and chemical structure, *J. Am. Chem. Soc.* **1964**, *86*, 1616–1626.

Biographies

Akinori Hirashima, Ph.D., is associate professor of pesticide chemistry at the Kyushu University at Fukuoka, Japan. Dr. Hirashima investigates the structural design of octopamine agonists. After obtaining a Ph.D. degree in the synthesis and stereochemistry of organophosphorus insecticides from the Kyushu University at Fukuoka, Dr. Hirashima undertook postdoctoral research with Professor John E. Casida at the Environmental Chemistry and Toxicology

Laboratory at the University of California at Berkeley. More recently, Dr. Hirashima has collaborated on projects with Professor Hans-J. Riebel from the Chemistry Department at the Bayer AG.

Tomohiko Eiraku is graduate student of pesticide chemistry at the Kyushu University at Fukuoka, Japan. Mr. Eiraku investigates inhibitors of calling behavior and *in vitro* pheromone biosynthesis using structural design.

Eiichi Kuwano, Ph.D., is professor of pesticide chemistry at the Kyushu University at Fukuoka, Japan. Dr. Kuwano investigates the structural design of juvenile–hormone agonists. After obtaining a Ph.D. degree in synthesis of *s*-triazine derivatives from amino acids and peptides and their biological activities from the Kyushu University at Fukuoka, Dr. Kuwano undertook postdoctoral research with Professor T. Roy Fukuto at the Department of Entomology at the University of California at Riverside. More recently, Dr. Kuwano has collaborated on projects with Professor Bruce D. Hammock of the Department of Entomology at the University of California at Davis.

Eiji Taniguchi, Ph.D., is emeritus professor of pesticide chemistry at the Kyushu University at Fukuoka, Japan. Dr. Taniguchi investigates the structural design of natural product haedoxan. After obtaining a Ph.D. degree in separation and characterization of effective components in haedoxo from the Kyushu University at Fukuoka, Dr. Taniguchi undertook postdoctoral research with Professor G. A. White at the Research Institute, Canada Department of Agriculture at Ontario.

Morifusa Eto, Ph.D., is emeritus professor of pesticide chemistry at the Kyushu University at Fukuoka, Japan. Dr. Eto investigates the structural design of organophosphorus insecticides. After obtaining a Ph.D. degree in toxic cyclic phosphorus esters from the Kyushu University at Fukuoka, Dr. Eto undertook postdoctoral research with Professor John E. Casida at the Department of Entomology at the University of Wisconsin at Madison.